JOURNAL OF CATALYSIS **165,** 249–261 (1997)
ARTICLE NO. CA971482

The Preparation and Characterisation of Fe-Promoted Al_2O_3-Supported Rh Catalysts for the Selective Production of Ethanol from Syngas

R. Burch* and M. J. Hayes

Catalysis Research Centre, The University of Reading, Whiteknights, RG6 6AD, Reading, Berkshire, United Kingdom

Received June 19, 1996; revised September 6, 1996; accepted September 6, 1996

This paper describes the development of a selective alumina-supported rhodium catalyst for the synthesis of ethanol from high pressure (10 bar) CO/H_2 mixtures. It has been shown that selectivity to ethanol of up to 50% can be achieved with an alumina-supported Rh catalyst containing 2 wt% Rh and promoted by 10 wt% Fe. Characterisation of the Fe-promoted Al_2O_3-supported Rh catalysts with increasing promoter loadings by selective chemisorption and temperature-programmed reduction (TPR) has provided evidence of a close interaction between the active metal and the promoter oxide especially at higher promoter loadings. The results obtained are consistent with the buildup of a close packed monolayer of the promoter oxide on the support surface which is possible due to the presence of a high surface density of hydroxyl groups on alumina. The influence of the metal precursor and the drying rate on the final metal salt distribution through the pore structure of a preshaped alumina support has also been investigated. It has been shown that impregnation of 1/16″ γ-alumina extrudates with an aqueous solution of iron nitrate causes the iron salt to be deposited at the outer edge of the pore structure. A more uniform distribution can be obtained if a methanolic solution of $Fe(NO_3)_3$ or an aqueous solution of an organometallic complex is used as the deposited metal precursor.

INTRODUCTION

Since the pioneering work of the Union Carbide research team in 1975, the ability of oxide-supported Rh catalysts to selectively produce oxygenated products from synthesis gas (syngas) (CO/H_2) mixtures has been recognised (1–3). It has been noted that the product distribution obtained from syngas reaction over a supported rhodium catalyst can be significantly altered by changing either the reaction conditions or the nature of the catalyst system. Modification of the catalyst by the judicious choice of support (4–15) and promoter materials (3, 12, 16–30) has been shown to significantly improve the performance of the system.

Recent work by Wachs and co-workers (31, 32) on the formation of atomically dispersed two-dimensional metal oxide overlayers when one metal oxide is deposited on a second metal oxide substrate has shown that these supported metal oxide species are formed by direct titration of surface hydroxyl groups of the high surface area support by the deposited metal oxide. Evidence for the removal of surface hydroxyls by this process can be seen from *in situ* infrared studies of the catalysts which show the disappearance of bands in the characteristic hydroxyl stretching frequency of the spectrum with increasing surface coverage (33).

The consumption of support surface hydroxyls can also be monitored by CO_2 chemisorption (33). At higher loadings of the deposited surface metal oxide infrared bands characteristic of species resulting from CO_2 chemisorption are seen to decrease and disappear completely at monolayer coverage.

It is therefore evident that a necessary condition for the buildup of a surface metal oxide overlayer is the presence of reactive surface hydroxyls on the oxide support. Oxide supports such as Al_2O_3, TiO_2, ZrO_2, and Nb_2O_5 possess a high surface density of reactive surface hydroxyls and tend to form a close packed monolayer of the supported metal oxide phase. SiO_2 possesses a much lower density of reactive surface hydroxyl groups and, consequently, does not form this close packed layer of the surface metal oxide phase (Table 1 in Ref. (31)).

Characterisation of promoted rhodium catalysts by techniques such as chemisorption, temperature-programmed reduction (TPR), and *in situ* FTIR spectroscopy has clearly demonstrated the importance of a close interaction between promoter and active metal in the development of a selective oxygenate synthesis catalyst (10–24, 27, 28, 34–36). This close interaction leads to an increased rhodium–promoter interface which is thought to accommodate chemisorbed CO which is carbon-bound to a rhodium atom and oxygen-bound to a promoter ion. This mode of CO adsorption is thought to be paramount in the catalytic synthesis of oxygenates from CO/H_2 mixtures (13, 18, 37–45).

In order to optimise this interaction it was thought that use of a support which could produce a close packed layer of deposited metal oxide would be advantageous. As can be seen from the available literature much of the work carried out to date has focussed on the development of a SiO_2-supported system. It was, therefore, decided to investigate

0021-9517/97 $25.00

the potential of γ-Al_2O_3 as a support for oxygenate synthesis catalysts.

Unpromoted alumina-supported Rh has, however, been shown to be a poor C_2-oxygenate synthesis catalyst exhibiting high selectivities to hydrocarbon products with methanol being the primary oxygenate observed (3, 9, 20). Vannice did not observe the synthesis of any oxygenate products from the reaction of various ratios of CO and H_2 over an unpromoted catalyst containing 1 wt% Rh supported on alumina (46). For this reason, interest in the system seems to have waned and literature precedents for work on oxide-promoted alumina-supported Rh catalysts is sparse (12, 20).

Evidence from experiments carried out on SiO_2-supported Rh catalysts suggests that addition of even a small amount of iron to the system has the effect of dramatically increasing the observed selectivity to ethanol (3, 15, 27). Iron-promoted SiO_2-supported Rh catalysts have also been shown to be highly efficient for the hydrogenation of acetaldehyde which is thought to be an important secondary reaction in the catalytic production of ethanol from synthesis gas (47).

It was envisaged, from results presented by Wachs *et al.* (31), that monolayer coverage of the alumina support would occur at a level equivalent to 0.58 mmol of deposited metal oxide per 100 m^2 of support. In the case of Fe_2O_3, this would equate to 17 wt%, or 11.7 wt% Fe. A direct consequence of this was thought to be the necessity to use a large promoter loading in order to generate the desired interaction between active phase and promoter. Catalysts containing nominal surface Fe loadings of between 0 and 14 wt% and a constant nominal Rh surface loading of 2 wt% were prepared during the course of this study.

The effect of promoter loading on catalytic activity and selectivity over an alumina-supported Rh catalyst under synthesis gas reaction conditions is described in this paper and rationalisation of the observed trends is aided by surface characterisation techniques such as H_2 and CO chemisorption and temperature-programmed reduction (TPR). The precautions taken and the techniques employed during the preparation of these catalysts are also described in light of the recent assertion by Wachs and coworkers (31, 48) that the structure and reactivity of the supported metal oxide phase is not dependent on the preparation method. This conclusion contrasts with much of the available data on the preparation of catalysts by impregnation into preshaped supports. It has been shown, for example, that a variety of different distributions of the deposited metal can be achieved by varying the impregnation conditions (49, 50).

The impregnation of aqueous and non-aqueous iron precursors into the pore structure of preshaped (1/16″) alumina extrudates was monitored and the final distributions related to the catalyst activity results obtained from crushed and sieved Rh catalysts prepared from similar precursors.

EXPERIMENTAL

Catalyst Preparation

The alumina used as a catalyst support throughout this study was a commercially available high purity (>99.94%) γ-Al_2O_3 supplied by Akzo Chemie. Its BET surface area and pore volume were measured as 190 ± 5 m^2 g^{-1} and 0.6–0.7 cm^3 g^{-1}, respectively. Extrudates (1/16″) were used as support material in experiments to confirm that a satisfactory distribution of the deposited iron oxide could be obtained from a particular precursor. Catalyst samples which were to be used for activity testing were prepared using support material which had previously been crushed and sieved to give a particle size of 250–600 μm.

Prior to impregnation the alumina was dried at 300°C for 2 h in order to expel any residual water from the pore structure. The support was subsequently cooled to room temperature in a desiccator and contacted with the appropriate concentration impregnating solution for up to 3 h. The iron oxide promoter was deposited either from a solution of iron nitrate in methanol or from an aqueous solution of NH_4[Fe(EDTA)] prepared in accordance with the method outlined by Stobbe *et al.* (51).

The promoter support phases were dried at 120°C overnight before final air calcination at 500°C for 4 h in a muffle furnace. A 0.5 g sample of each of these phases was retained for activity measurement to investigate if any of the observed CO hydrogenation activity of the final catalysts is due to the inherent activity of alumina-supported iron oxide.

Introduction of rhodium to the system was achieved by sequential dry impregnation of the relevant promoter oxide-support phase with either an aqueous solution of $Rh(NO_3)_3$ or a solution of $Rh(acac)_3$ in toluene. The binary systems thus produced were dried in a 120°C oven overnight before being finally air calcined for 4 h at 500°C.

The nomenclature of *x*Rh/*y*Fe/Al is used throughout this paper to denote an alumina-supported catalyst containing *x* wt% Rh promoted by *y* wt% Fe.

Catalyst Activity Measurement

The activity of the catalysts for the synthesis gas reaction and the selectivity to the various products was determined using a high pressure (10 bar) flow microreactor system. The flows of carbon monoxide and hydrogen, which were provided from compressed cylinders, were controlled by digital Bronkhorst High Technology Series model F-100/200 mass flow controllers.

The catalyst sample (150 mg) was placed in the centre of a glass-lined stainless steel reactor (0.25″ O.D.) which was mounted horizontally in a furnace. The reactor pressure

was governed by a back pressure regulator (Tescom Corporation Series 26-1700) which was located downstream. A 100 mg bed of 10 Å molecular sieve was placed upstream of the catalyst in order to trap any unwanted $Fe(CO)_5$ species, which may originate from the CO cylinder. Removal of this trap has been shown by Burch and Petch (27) to substantially alter the product distribution obtained when an unpromoted SiO_2-supported Rh catalyst is exposed to synthesis gas.

Downstream of the back pressure regulator the reactor effluent passed through a short length of stainless steel tubing to the gas sampling valve of a Perkin Elmer 8500 series gas chromatograph. To avoid condensation of nonvolatile products, all of the tubing downstream of the reactor was heated to 150°C. Product separation was achieved by means of a Reoplex precolumn (which preferentially retains oxygenates over hydrocarbons) connected in series with a Porapak QS column. Eluents from the Porapak column were quantified by means of a calibrated flame ionization detector. The chromatographic system was interfaced with a PE Nelson 950 series integrator and Amstrad 1512 personal computer in order to automate data handling.

Catalyst samples were exposed to an *in situ* H_2 (20 cm^3 min^{-1}) prereduction at 300°C for 2 h. The reactor temperature was lowered to 270°C and the gas flow changed to 20 cm^3 min^{-1} of a 1 : 1 CO/H_2 mix prior to pressurisation of the system to 10 bar. The catalyst was allowed to reach steady state (ca. 2 h on stream) before analysis of the first sample of the reaction products.

Catalyst Characterisation

Electron microscopy—SEM and AEM. The distribution of deposited iron oxide species through the pore structure of a preshaped alumina support has been characterised by the techniques of scanning electron microscopy (SEM) and analytical electron microscopy (AEM) using a JEOL model 840 scanning electron microscope coupled to a LINK AN10000 analyser.

When carrying out an SEM experiment the preshaped sample was initially split to expose its cross-section, then coated in either carbon or gold, and finally mounted on an SEM stub using epoxy resin. The electron beam of the microscope was concentrated to a small probe (1–20 nm in diameter) and was scanned across the surface of the sample.

H_2 and CO chemisorption. The dispersion of rhodium in the unpromoted and promoted catalysts was measured by chemisorption of hydrogen and CO in a conventional glass volumetric system, at pressures of up to 10 Torr (1 Torr = 133.3 Pa). The results obtained provided valuable information on the effect of promoter loading on the chemical environment of the active metal. The catalyst sample was prereduced in H_2 (0.8 bar) at 300°C for 2 h. These reduction conditions were intended to replicate those employed during catalyst activity measurement.

At the end of the reduction period the system was again outgassed and allowed to cool to room temperature under vacuum. A known pressure of H_2 was then admitted into the dosing volume and subsequently expanded into the sample volume. The value of the equilibrium pressure was noted. This step was repeated up to 10 times until the dosing pressure was approximately 10 Torr.

Cleaning of the surface was carried out by repeating the outgassing step and the CO adsorption isotherm was measured in an identical manner to that described above. Upon completion, the system was outgassed again and the CO isotherm repeated. This second isotherm measured the amount of weakly adsorbed CO which had been lost during the outgassing step. The amount of more strongly adsorbed CO was estimated by subtraction. The amount of gas adsorbed, in terms of H atoms or CO molecules, was obtained by extrapolating the linear part of the relevant isotherm to zero pressure (52).

Temperature-programmed reduction (TPR). TPR characterisation of the catalysts used in this study provided interesting information on the effect of promoter loading on the ease of reducibility of both the noble metal oxide and the promoter oxide.

In order to generate a TPR profile 50 mg of the sample under investigation was placed in a horizontally mounted silica reactor and secured in the centre of a furnace. The sample was exposed to a 10 cm^3 min^{-1} flow of 5% H_2/Ar which had passed through the reference channel of a thermal conductivity detector and the temperature ramped at 10°C min^{-1} from room temperature to 700°C.

After passing over the sample the depleted reductant gas flowed through the dry ice cold trap to remove any H_2O formed as a reaction product and finally to the analytical channel of the detector. The difference in H_2 partial pressure between the two sides of the detector produced a difference in the resistance of the filaments, giving rise to a voltage signal which was amplified and sent to a PE Nelson 950 series integrator and PC data handling system.

RESULTS

Catalyst Preparation

Line a in Fig. 1 shows the radial profile which is observed when a predried alumina support in the form of 1/16″ extrudates is impregnated with an aqueous solution of iron nitrate (pH < 2) of the appropriate concentration and examined by scanning electron microscopy. This profile is referred to as pellicular or "eggshell" and describes a situation where the active ingredient has been deposited towards the outer edge of the support pore structure. Comparison of the integrated areas shown in Fig. 1, lines a and b, respec-

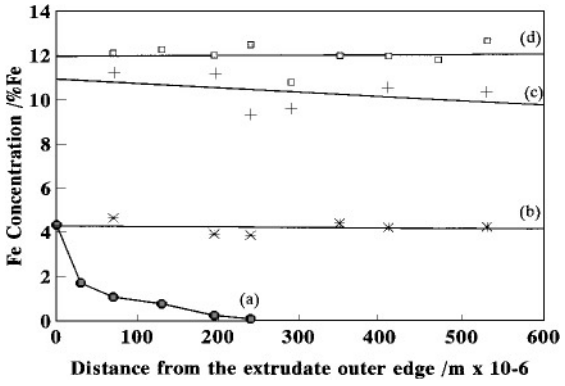

FIG. 1. Variation of Fe concentration with distance from the outer edge of a 1/16″ alumina extrudate for (a) an Al_2O_3-supported Fe phase containing 4 wt% Fe prepared by impregnation with aqueous $Fe(NO_3)_3$, (b) a 4 wt% Fe on alumina system prepared by aqueous impregnation with NH_4[Fe(EDTA)], (c) an alumina-supported Fe system containing 10 wt% Fe deposited from a methanolic solution of $Fe(NO_3)_3$, and (d) a 10 wt% Fe on alumina phase prepared by aqueous impregnation with NH_4[Fe(EDTA)].

tively, suggests that much of the $Fe(NO_3)_3$ deposited from the aqueous solution is deposited on the outer surface of the pellet.

It was observed that if the impregnation was carried out under conditions of incipient wetness the "eggshell" was formed almost immediately and extending the contact time between the support and the impregnating solution had very little effect on the final observed profile. If, however, the volume of this solution was greater than that of the support then extending the contact time had the effect of extending the eggshell and ultimately producing a uniform distribution of adsorbate. Examination of a cross-section of an extrudate by SEM and AEM after drying showed, however, that the drying procedure had the effect of regenerating the eggshell radial profile.

Line c shows that a more uniform distribution of the deposited metal oxide can be achieved when a methanolic solution of iron nitrate is used as the impregnating liquid. A uniform distribution yields the minimum surface concentration for a given loading of adsorbate. Following the work of Stobbe *et al*. (51) on the preparation of uniformly distributed iron oxide on preshaped MgO, an aqueous solution of NH_4[Fe(EDTA)] (pH = 5.5) was prepared and used as the impregnant to our predried alumina extrudates. Lines b and d of Fig. 1 show typical Fe_2O_3 distributions obtained using this technique. Line d suggests a uniform surface distribution of 12 wt% Fe for a system which is nominally referred to as containing 10 wt% Fe. This discrepancy may be due to the fact that preparation of this system involved five successive impregnations. This was necessary due to the solubility of NH_4NO_3 which is formed as a side product in the preparation of the NH_4[Fe(EDTA)] complex which limits the amount of the Fe precursor which can be present in the impregnating liquid (51). Some of the observed error may also be associated with the fact that SEM and AEM are not bulk techniques.

Preparation of Al_2O_3-supported iron oxide phases by this method is complicated by the inherent explosiveness of the NH_4NO_3, produced as a side-product in the preparation of the Fe precursor, which causes the extrudates to burst under calcination!

Catalytic Activity in CO/H_2 Reactions

Catalytic activity results are presented for two series of alumina-supported Fe-promoted Rh catalysts containing Fe promoter loadings of between 0 and 14 wt% (Fig. 2). The Rh content in all cases was 2 wt%. The Fe promoter was deposited on both sets of catalysts from an appropriate concentration solution of iron nitrate in methanol. The Rh active phase was deposited either from a solution of $Rh(acac)_3$ in toluene or an aqueous solution of $Rh(NO_3)_3$. Activity data are also presented for a catalyst containing 10 wt% Fe from an aqueous NH_4[Fe(EDTA)] solution. Aqueous $Rh(NO_3)_3$ was used as the active phase precursor for this system. It can be clearly seen in Fig. 2 that CO conversion increases with increasing promoter loading up to a level approaching monolayer coverage (ca. 10 wt%) (31). Further increase of the Fe promoter loading to 14 wt% Fe (equivalent to 20 wt% Fe_2O_3) is shown to have an adverse effect on overall catalytic activity. It also appears from the results presented here that the influence of the respective metal precursors used during catalyst preparation on the final catalyst activity is quite slight.

Some deactivation resulting from coke formation on the catalyst surface was observed after prolonged exposure to

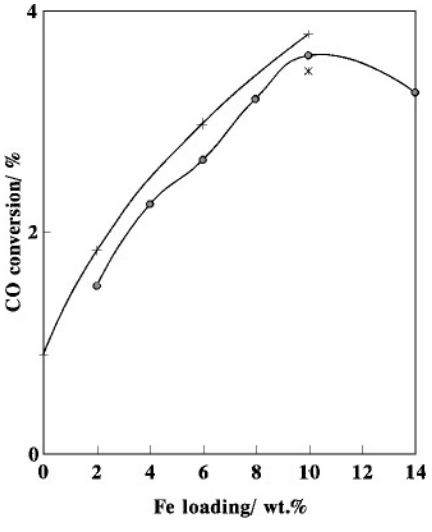

FIG. 2. Plot showing the influence of increasing Fe-promoter loading on CO conversion over Al_2O_3-supported Rh catalysts which have been prepared from different metal precursors and which have subsequently been exposed to 20 cm^3 min^{-1} of 1 : 1 CO/H_2 at 270°C and 10 bar for 2 h. (•) $Rh(acac)_3$ in toluene, (+) aqueous $Rh(NO_3)_3$, and (∗) NH_4[Fe(EDTA)].

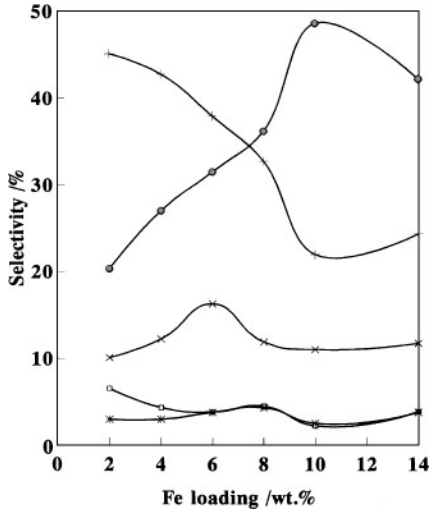

FIG. 3. The effect of increased Fe-promoter loadings on the observed product selectivities over a series of Al_2O_3-supported Rh catalysts prepared from $Rh(acac)_3$ in toluene which have been exposed to 20 cm^3 min^{-1} of 1 : 1 CO/H_2 at 270°C and 10 bar for 2 h. (•) C_2H_5OH, (+) CH_4, (∗) C_2 hydrocarbons, (□) C_3 hydrocarbons, and (×) CH_3OH.

the reactant gases. CO conversion over the catalyst containing 10 wt% Fe and prepared from aqueous $Rh(NO_3)_3$ and $Fe(NO_3)_3$ in methanol was found to decrease from 3.8% after 2 h exposure to the reaction conditions to 3.1% after 4.5 h.

The relationship between promoter loading and selectivity to specific products is given in Figs. 3 and 4. Rates of conversion of CO and formation of ethanol for the respective catalyst series are given in Table 1. All of the catalysts show an encouraging trend toward suppression of methane

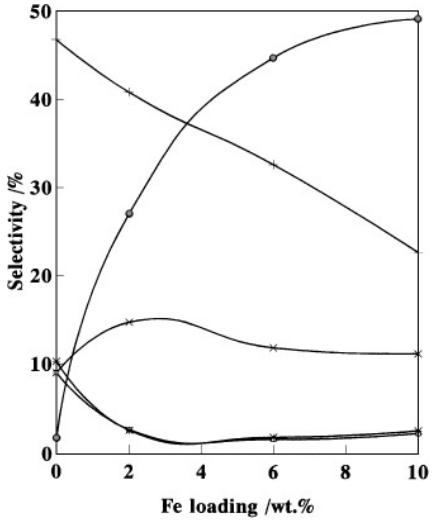

FIG. 4. The effect of increased Fe-promoter loadings on the observed product selectivities over a series of Al_2O_3-supported Rh catalysts prepared from aqueous $Rh(NO_3)_3$ which have been exposed to 20 cm^3 min^{-1} of 1 : 1 CO/H_2 at 270°C and 10 bar for 2 h. (•) C_2H_5OH, (+) CH_4, (∗) C_2 hydrocarbons, (□) C_3 hydrocarbons, and (×) CH_3OH.

TABLE 1

Catalytic Activity Results for Al_2O_3-Supported Fe-Promoted Rh Catalysts after 2 h Exposure to Reaction Conditions

	$Rh(acac)_3$/toluene $Fe(NO_3)_3$/MeOH	$Rh(NO_3)_3$ (aq.) $Fe(NO_3)_3$/MeOH
2Rh/2Fe/Al	CO conv. 41.9 (1.5%)	50.8 (1.8%)
	EtOH Form^n 4.26	6.87
2Rh/4Fe/Al	62.5 (2.3%)	
	8.44	
2Rh/6Fe/Al	73.6 (2.7%)	82.7 (3.0%)
	11.6	18.5
2Rh/8Fe/Al	88.9 (3.2%)	
	16.1	
2Rh/10Fe/Al	99.7 (3.6%)	105.0 (3.8%)
	24.2	25.7
2Rh/14Fe/Al	90.3 (3.3%)	
	19.0	

Note. CO conversion is given as μmol CO conv. g_{cat}^{-1} min^{-1}. Numbers in parentheses give the %CO converted. EtOH formation is given as μmol EtOH formed g_{cat}^{-1} min^{-1}.

selectivity coupled to an enhanced ethanol selectivity as the Fe-promoter loading increases. Ethanol selectivities approaching 50% can be obtained after 2 h exposure to the reactant gases from all the catalysts containing 10 wt% Fe.

Selectivity to methane decreases from approximately 50% over the catalysts containing 2 wt% Fe to less than 25% over the catalysts containing 10 wt% Fe. It is also interesting to note that in the case of the 2Rh/14Fe/Al catalyst prepared from $Rh(acac)_3$ in toluene and a methanolic solution of $Fe(NO_3)_3$ the elevated Fe loading has the effect of suppressing the ethanol selectivity slightly. The effect is mirrored by a corresponding increase in the methane selectivity. This result tends to suggest that there is a limit beyond which any increase in promoter loading is no longer beneficial.

Chemisorption Measurements

The problems associated with the use of selective chemisorption to quantify adsorption on more highly dispersed systems are illustrated in Fig. 5 which shows the H_2 and CO isotherms obtained for an unpromoted Rh (2 wt%) on alumina (CK300). The molar ratio of CO adsorbed : H_2 adsorbed approaches 4. If the usual adsorbate : metal stoichiometries are taken (i.e., 1/2 in the case of H_2 and 1 in the case of CO) then the percentage of Rh dispersion works out as 53% if the H_2 adsorption data are taken and 95% according to the CO isotherm. The Rh metal surface area and mean Rh particle diameter (assuming a spherical geometry) are calculated to be 4.7 m^2 g^{-1} and 2.1 nm respectively from the H_2 data compared with 8.4 m^2 g^{-1} and 1.1 nm respectively from the CO isotherm.

It is clear from such discrepancies that it is a gross oversimplification to assume an H atom or CO molecule : Rh atom stoichiometry of 1 in this instance. The occurrence of

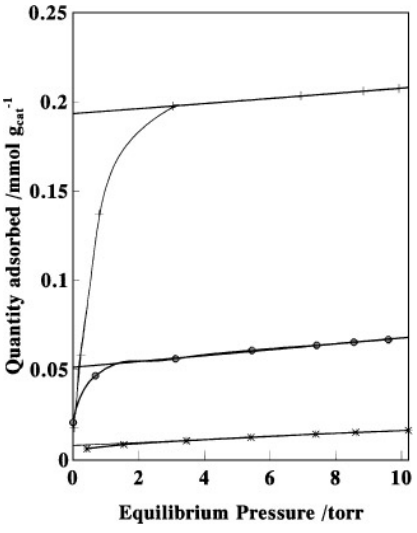

FIG. 5. The room temperature isotherms for the adsorption of H_2 and CO onto a prereduced unpromoted Al_2O_3-supported Rh catalyst. (•) H_2, (+) CO, and (∗) weakly adsorbed CO.

apparent multiple adsorption of CO at the dilute end of the Rh surface concentration range in Rh/Al_2O_3 systems has been reported previously (53, 54). Infrared spectral evidence has supported the idea of a doublet of CO molecules adsorbed on a single Rh site (55, 56). The multiple adsorption has been attributed to the existence of linear and bridged CO bonding and it has been observed that the limiting CO molecule to surface Rh atom stoichiometry is 2 (57). It would seem that in our case the values obtained for active metal dispersion, surface area, and mean particle size calculated from the hydrogen adsorption data are more reliable.

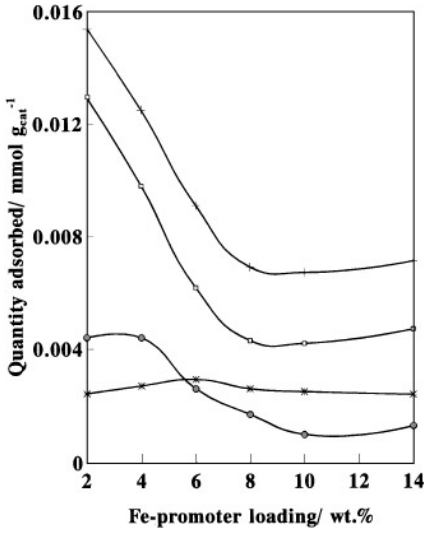

FIG. 6. The relationship between room temperature chemisorption capacity and promoter loading for a series of Al_2O_3-supported Rh catalysts prepared from $Rh(acac)_3$ in toluene. (•) H_2, (+) total CO, (□) strongly adsorbed CO, (∗) weakly adsorbed CO.

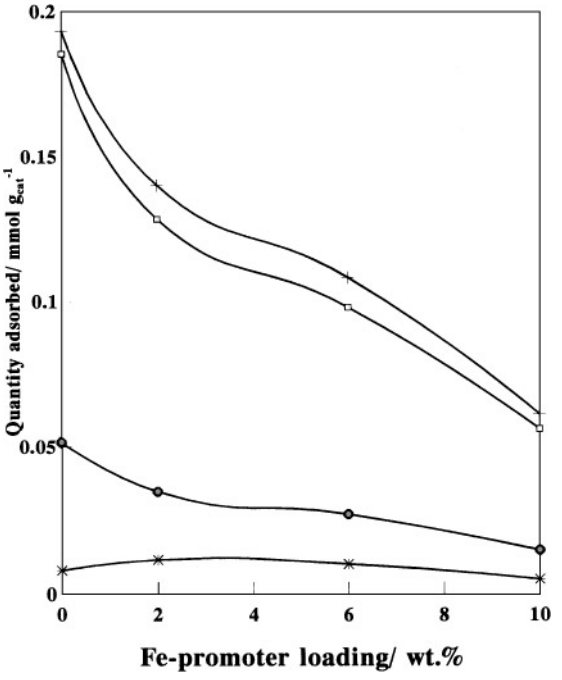

FIG. 7. The relationship between room temperature chemisorption capacity and promoter loading for a series of Al_2O_3-supported Rh catalysts prepared from aqueous $Rh(NO_3)_3$. (•) H_2, (+) total CO, (□) strongly adsorbed CO, (∗) weakly adsorbed CO.

A trend towards diminished chemisorption capacity with increased promoter loading is seen in both series of alumina-supported catalysts (Figs. 6 and 7). Comparison of Tables 2 and 3 shows that the H_2 or CO chemisorption capacity for any given catalyst where the aqueous $Rh(NO_3)_3$ is used as the active phase precursor is up to 10 times greater than that displayed by the corresponding catalyst prepared from $Rh(acac)_3$ in toluene. The amount of adsorbate taken up by these latter catalysts (especially those with higher promoter loadings as is evident from Table 3) is not sufficiently greater than the intrinsic error associated with using the technique for the results to be regarded as a reliable basis for the calculation of active phase dispersions or particle size values.

It is interesting to note, however, that this small amount of adsorption of CO and H_2 is not coupled to a significant decrease in catalytic activity under high pressure conditions. This point will be discussed in more detail later.

TABLE 2

CO and H_2 Chemisorption Data for Al_2O_3-Supported Catalysts Prepared from $Rh(NO_3)_3$ (aq.) and $Fe(NO_3)_3$/MeOH

Catalyst	H_2 ads./mmol g_{cat}^{-1}	CO ads./mmol g_{cat}^{-1}
2Rh/Al	0.051	0.185
2Rh/2Fe/Al	0.035	0.140
2Rh/6Fe/Al	0.027	0.110
2Rh/8Fe/Al	0.015	0.061

TABLE 3

CO and H_2 Chemisorption Data for Al_2O_3-Supported Catalysts Prepared from $Rh(acac)_3$/Toluene and $Fe(NO_3)_3$/MeOH

Catalyst	H_2 ads./mmol g_{cat}^{-1}	CO ads./mmol g_{cat}^{-1}
2Rh/2Fe/Al	0.004	0.015
2Rh/4Fe/Al	0.004	0.013
2Rh/6Fe/Al	0.004	0.009
2Rh/8Fe/Al	0.002	0.007
2Rh/10Fe/Al	0.001	0.007
2Rh/14Fe/Al	0.001	0.007

Temperature Programmed Reduction

Figure 8 shows the TPR profiles obtained for an unpromoted alumina-supported Rh (2 wt%) catalyst and for a similar system containing 2 wt% Fe. The characteristic profile for the unpromoted system consists of a broad band representing the consumption of hydrogen throughout the temperature region 100–570°C. This result was quite surprising and was in sharp contrast with the profile obtained for an equivalent catalyst containing 2 wt% Fe which displayed a single sharp peak for Rh reduction at approximately 150°C. It also disagreed with the findings of Prins and co-workers (58, 59) who have shown TPR profiles for fresh but uncalcined alumina-supported Rh catalysts which show a single sharp reduction feature at approximately 150°C. The result is, however, consistent with the findings of Yao and co-workers (53) who observed a similar profile for an unpromoted alumina-supported Rh catalyst which had been exposed to a high temperature oxidation (equivalent to our calcination). The difficulty in effecting reduction is attributed to interaction of Rh-oxide with the support at elevated temperature (53, 60).

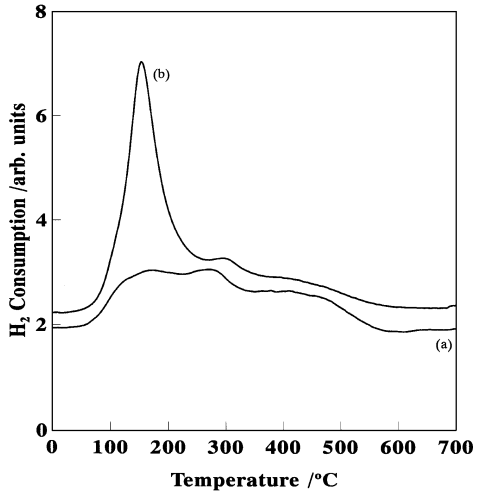

FIG. 8. TPR profiles of Al_2O_3-supported Rh catalysts prepared from aqueous $Rh(NO_3)_3$ and exposed to a 10°C min^{-1} temperature ramp from room temperature to 700°C in a 10 cm^3 min^{-1} flow of 5% H_2/Ar. (a) 2Rh/Al, (b) 2Rh/2Fe/Al.

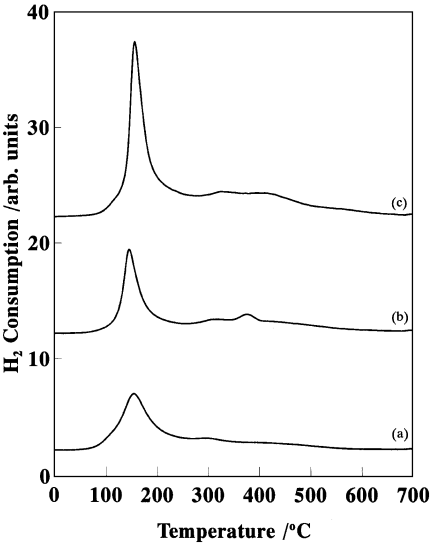

FIG. 9. TPR profiles of Al_2O_3-supported Rh catalysts prepared from aqueous $Rh(NO_3)_3$ and exposed to the same reduction conditions as those described in Fig. 11. (a) 2Rh/2Fe/Al, (b) 2Rh/6Fe/Al, (c) 2Rh/10Fe/Al.

This phenomenon is prevented from occurring in the case of the Fe-promoted catalyst as a result of the order of impregnation which was favoured during catalyst preparation and so in that case the features attributable to Rh reduction in the observed TPR profile are more consistent with the findings of Prins and co-workers (58, 59). Characteristic TPR profiles for the Fe-promoted series of catalysts where the Rh active phase has been deposited from an aqueous solution of $Rh(NO_3)_3$ are shown in Fig. 9. Figures 10 and 11

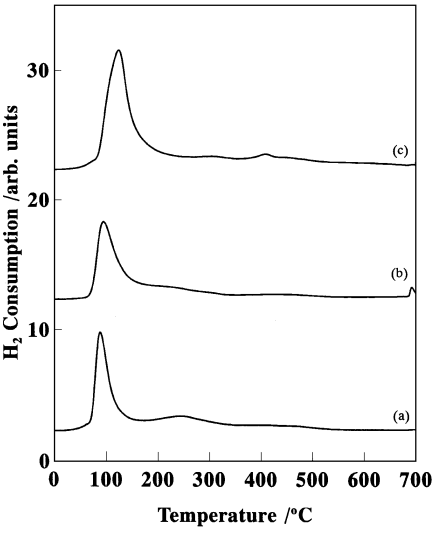

FIG. 10. TPR profiles of Al_2O_3-supported Rh catalysts prepared from $Rh(acac)_3$ in toluene. Reduction is as described in Fig. 11. (a) 2Rh/2Fe/Al, (b) 2Rh/4Fe/Al, (c) 2Rh/6Fe/Al.

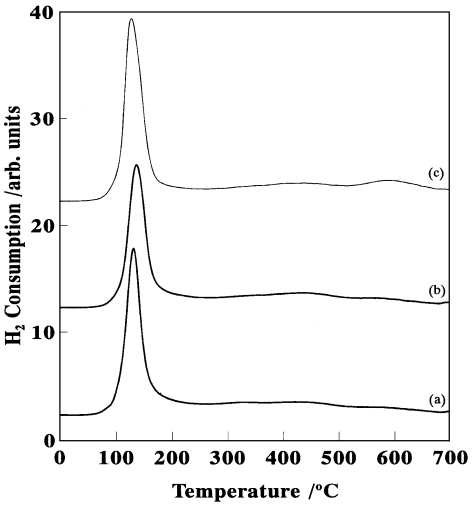

FIG. 11. TPR profiles of Al_2O_3-supported Rh catalysts prepared from $Rh(acac)_3$ in toluene. Reduction is as described in Fig. 11. (a) 2Rh/8Fe/Al, (b) 2Rh/10Fe/Al, (c) 2Rh/14Fe/Al.

show the corresponding profiles the catalysts derived from $Rh(acac)_3$ in toluene. The profiles display a sharp Rh reduction peak in the 100–150°C region irrespective of promoter loading or active phase precursor. Despite elevated Fe promoter loadings no sharp peak is seen to develop in the higher temperature region which would be deemed characteristic of Fe reduction.

It is interesting to note, however, that the area of the peak in the 100–150°C region which previously had been ascribed solely to Rh reduction is seen to increase with increasing promoter loading and becomes representative of a much larger hydrogen consumption than that required to

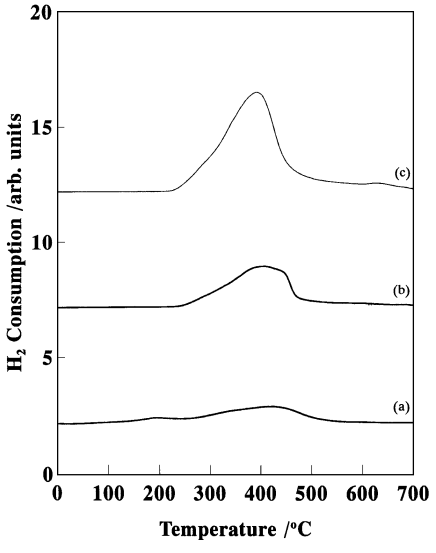

FIG. 12. TPR profiles of Al_2O_3-supported Fe_2O_3 phases generated during a reduction similar to that described in Fig. 11. (a) 2Fe/Al, (b) 6Fe/Al, (c) 10Fe/Al.

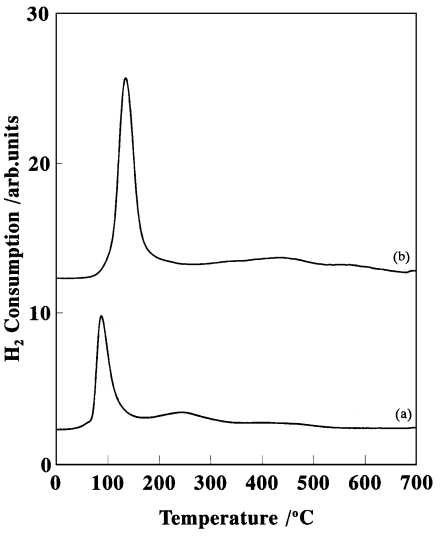

FIG. 13. Comparison of characteristic Rh reduction temperature for Al_2O_3-supported catalysts promoted by 2 and 10 wt% Fe respectively: (a) 2Rh/2Fe/Al and (b) 2Rh/10Fe/Al.

achieve complete reduction of any Rh_2O_3 present. It would seem, therefore, that the presence of Rh has the effect of accelerating the reduction of the iron oxide moiety.

Comparison with Fig. 12 which shows the TPR profiles for alumina-supported iron oxide systems in the absence of Rh reveals that sequential impregnation of Rh from either precursor has the effect of reducing the temperature at which iron oxide reduction occurs by up to 250°C.

Figure 13 compares the TPR profiles obtained for catalysts containing 2 wt% Fe and 10 wt% Fe prepared from $Fe(NO_3)_3$ in methanol and $Rh(acac)_3$ in toluene. It can be seen quite clearly that the temperature at which the dominant reduction peak occurs increases by up to 50°C with increasing promoter loading. The large difference in peak area alluded to earlier is also evident. A rationalisation for these observations will be furnished in the discussion section.

DISCUSSION

The investigations into the effect of metal precursor on the final distribution of deposited metal oxide on preshaped γ-alumina revealed some very interesting results. From Fig. 1, line a, it can be seen that impregnation of the support with an appropriate concentration solution of iron nitrate forms a system which reveals a pellicular or "eggshell" radial profile of the deposited salt. It is clear that the active phase precursor has been deposited towards the outer edge of the support with little evidence for penetration of the pore structure.

In the case of incipient wetness impregnation of a predried support (where the volume of the impregnating liquid is just sufficient to fill the pores) the impregnant is

transported to the interior of the support as the result of capillary suction. However, in the case of imbibition of an aqueous solution of $Fe(NO_3)_3$ into the pore structure, interaction of the Fe^{3+} ions with the hydroxylated support results in the formation of insoluble $Fe(OH)_3$ which precipitates around the outer edge of the pore structure and is thus prevented from migrating further. This gives rise to the inhomogeneous distribution of Fe which is observed from this precursor. A similar observation was made by Stobbe *et al*. while studying the preparation by impregnation of iron oxide catalysts supported on preshaped MgO (51).

Increasing the volume of the impregnating solution and extending the time of contact of the solution with the support had the effect of extending the eggshell. After a contact time of approximately 3 h a cross-section through a typical extrudate (prior to drying) revealed a radial profile which was characteristic of a uniform distribution of the impregnant. If the volume of impregnating solution is sufficiently in excess of the pore volume an extended contact time has the effect of setting up an adsorption–desorption equilibrium between the pore walls of the support and the bulk of the solution. This effect, which can be likened to that which occurs in liquid chromatography, causes the solute to slowly diffuse towards the interior of the extrudate. This feature is only observed in the case of wet impregnation (where the support has been soaked in solvent prior to contact with the impregnating solution) or in the case of dry impregnation where the volume of the impregnating liquid is greater than the support pore volume.

The change of pellicular profiles to more closely resemble uniform profiles as the result of diffusional relaxation during an extended contact time has been observed previously for the impregnation of H_2PtCl_6 (61, 62) into preshaped alumina.

It was noted, however, that the drying step had the effect of reforming the eggshell even after an extended contact time and use of an excess of external solution. Komiyama *et al*. observed a similar effect while studying the impregnation of $NiCl_2$ into 4 mm diameter spherical γ-alumina pellets (63). The Ni salt was seen to be distributed uniformly prior to drying but the drying procedure (110°C for 2 h) had the effect of causing the $NiCl_2$ to accumulate towards the outer edge of the pellet. Intrapellet liquid movement during drying resulting in external segregation of the impregnant was envisaged as capillary flow (63, 64).

Komiyama *et al*. (63) have shown, however, that the uniform distribution of $NiCl_2$ on alumina is preserved if a heating rate of 600°C h^{-1} is employed during the drying step. It would, therefore, be expected that a uniform distribution could also be preserved if the drying conditions were not altered but the impregnant was dissolved in a more volatile solvent. To investigate this suggestion the impregnation of a methanolic solution of iron nitrate into 1/16″ γ-alumina extrudates was monitored. Figure 1, line c, shows the vast improvement in the homogeneity of distribution of the iron salt on the alumina support observed when methanol was used as a solvent. A uniform distribution of the iron salt throughout the support pore structure was observed, even after exposure of the system to drying conditions which were identical to those employed when the imbibed liquid consisted of an aqueous solution of iron nitrate, i.e., 120°C overnight.

Increasing the viscosity of the liquid in the pores should also prevent it from being forced outwards as the result of capillary forces experienced during drying. This can be done by using an organometallic complex exhibiting this property as the deposited metal precursor. Stobbe *et al*. (51) reported uniform distributions of impregnant on preshaped magnesium oxide pellets when an aqueous solution of either NH_4[Fe(EDTA)] or NH_4[Fe(OH)citrate] was used as the impregnating solution. Lines b and d of Fig. 1 show that very uniform distributions of Fe across a section of a typical 1/16″ γ-alumina extrudate can be obtained from an aqueous solution of NH_4[Fe(EDTA)]. The presence of NH_4NO_3 in the impregnating solution, however, has the effect of causing the pellets to burst under calcination. The technique of impregnation into preshaped supports has been the subject of thorough review by Komiyama (64) and Lee and Aris (65).

Figures 2–4 show the effect of promoter loading on the performance of crushed and sieved (250–600 μm) samples of iron-promoted alumina-supported Rh catalysts prepared from different precursors for CO hydrogenation at 270°C and 10 bar pressure. It can be seen from these plots that the use of different promoter and active metal precursors during the catalyst preparation procedure has little effect on final overall catalyst activity and selectivity to major products. This observation is in agreement with the work of Wachs *et al*. (31, 48) who have claimed, as a result of the characterisation of a variety of systems by laser Raman spectroscopy, that the structure and reactivity of the deposited metal oxide phase is not dependent on the preparation technique or the deposited metal oxide precursor.

The function of the promoter and the effect of an elevated loading can be elucidated from closer examination of the activity, selectivity, and characterisation data. It is known that a promoter can act passively by blocking the Rh surface, thereby suppressing reactions which require large ensembles of metal atoms (10, 12, 24). This will give rise to selectivity changes on exposure of the catalyst to the reaction conditions. However, the presence of the promoter can also result in the build-up of a new active site which may selectively produce a desired product. If both phenomena are operating simultaneously one would expect catalytic activity and selectivity to the desired reaction product to pass through a maximum with increasing promoter loading.

It can be seen from Fig. 2 that the activity of the catalysts for the CO hydrogenation reaction increases monotonically

with promoter loading up to a limiting value which occurs as the promoter coverage approaches a monolayer. Increasing the surface Fe-loading to 14 wt% causes a decrease in overall catalytic activity. This observation agrees with the findings of Prins and co-workers (12) which have shown that a vanadium-oxide-promoted alumina-supported catalyst containing 1.5 wt% Rh with a V/Rh ratio of 7.0 was marginally more active than the corresponding system with a V/Rh ratio of 8.4.

Bhore *et al*. (20) have not observed such a limiting value for promoter loading when studying molybdenum-promoted alumina-supported Rh catalysts. The results presented by this group reveal a higher catalytic activity for an alumina-supported catalyst containing 3 wt% Rh and 15 wt% Mo than for a system which contains a similar loading of Rh but only 7.5 wt% Mo. Interestingly, no data were presented for a catalyst system which contained a Mo loading intermediate between these two values.

Figures 3 and 4 show the effect of Fe-promoter loading on the selectivities to major products. It is immediately apparent that the ethanol selectivity curve is almost the exact mirror image of the methane selectivity curve in both cases. Increasing the Fe-promoter loading has the effect of increasing the selectivity to ethanol which is the primary C_2-oxygenate product observed from synthesis gas reaction over all these catalysts. The selectivity to methane decreases almost linearly with increasing Fe loading. This trend suggests that an increased promoter loading has the effect of increasing the number of active sites for oxygenate synthesis on the catalyst surface. This increase occurs primarily at the expense of the active site for methanation. It is also evident from Fig. 3 that increasing the Fe promoter loading to 14 wt% is no longer beneficial for oxygenate synthesis.

Figures 6 and 7 reveal a trend towards a suppression of chemisorption capacity with increased promoter loading. A decrease in chemisorption capacity is normally indicative of an increased Rh particle size. However, TEM studies carried out by Prins and co-workers on MoO_3- and V_2O_3-promoted Rh catalysts have shown that the Rh particle size is not greatly influenced by an increase in promoter loading (12, 19). This result is confirmed by recent XRD studies carried out by Shen *et al*. (66) on MoO-promoted SiO_2-supported Rh catalysts. No XRD peaks attributable to Rh were observed, which is consistent with a rhodium particle size of less than 2 nm.

A suppression of chemisorption capacity would also be expected with increased promoter loading if the promoter oxide or a significant proportion thereof is located on or adjacent to the active metal. This would cause the active metal to be "hidden" from the impinging gas phase adsorbate, leading to the observed decrease in chemisorption.

The promoter can be brought into close contact with the metal surface either during the impregnation step or during the reduction step. It has been shown that redissolution of V_2O_3 as $VOCl_2 \cdot 5H_2O$ during the impregnation of an acidic aqueous solution of $RhCl_3$ can result in coverage of the Rh active phase by V_2O_3 in the final V_2O_3-supported Rh catalyst (11, 67). In order to investigate if a similar effect was operating on the surfaces of our catalysts, a sample of an alumina-supported iron oxide phase (10 wt% Fe) was contacted with a dilute solution of nitric acid (0.1 *M*) for up to 2 h. Analysis of the aqueous external solution by atomic absorption spectrometry showed that no surface iron had been redissolved. This result suggests that surface decoration of the active metal by the promoter oxide does not occur during impregnation of the Rh precursor.

Suppression of chemisorption on noble metals supported on transition metal oxides such as TiO_2 and V_2O_3 after reduction at high temperatures (>450°C) was first observed by Tauster and Fung (68). This effect, termed strong metal support interaction (SMSI), has been reviewed thoroughly by Bond and Burch (69) and more recently by Haller and Resasco (70). Coverage of the noble metal by a transition metal suboxide such as Ti_4O_7, formed during the reduction step, is thought to be responsible for this effect (71, 72).

The temperature used to effect Rh reduction in the case of our catalysts (300°C) was substantially lower than the 450°C reduction temperature which was required before Fung and Tauster (68) observed suppression of chemisorption. Later work by Prins and co-workers (12, 19) has shown a systematic decrease in chemisorption capacity with increased promoter loading for V_2O_3- and MoO_3-promoted Rh catalysts even after reduction at 250°C.

Comparison of Figs. 6 and 7 shows that the extent to which a particular series of catalysts undergoes SMSI seems to be dependent on the active metal precursor. The catalysts prepared from $Rh(acac)_3$ in toluene show an almost complete suppression of chemisorption (Fig. 6) with the amount of CO or H_2 taken up by any particular catalyst in this series being an order of magnitude lower than the amount of adsorbate taken up by the corresponding catalyst prepared from an aqueous solution of $Rh(NO_3)_3$. Figures 2–4 show, however, that steady state catalytic activity or selectivity to oxygenate product seems to be independent of the extent to which SMSI has occurred.

The apparent absence of a relationship between the extent to which SMSI has taken place and the steady state activity for CO hydrogenation has been noted previously (9, 72–74). Morris *et al*. (74) have indicated that the CO/H_2 reaction itself has the effect of at least partially reversing the SMSI effect. Oxygen (formed from dissociated CO) and water (formed as a reaction product) have been shown to restore the chemisorption properties of the metal (74). It is therefore claimed that a steady state in activity and selectivity is achieved after a certain time period and so the effect of a severely reduced chemisorption capacity is no longer evident when the first sample of the reactor effluent gas is analysed (24).

However, the fact that the steady state activity for the production of oxygenates remains much higher than would be the case for an unpromoted system suggests that a close interaction between Rh and promoter oxide still remains and that the surface modifications which occurred during the reduction step have not been completely reversed. A similar conclusion has been reached by Ponec and co-workers when considering enhancement of the rate of oxygenate production over a V_2O_3-promoted SiO_2-supported Rh catalyst (24).

It has been shown that the chemisorption capacity of a catalyst which has undergone SMSI can be completely regenerated if the catalyst, operating at steady state in a CO/H_2 flow, is flushed with hydrogen and then rereduced at 200°C for 1 h (75).

Further evidence for the existence of a close interaction between active phase and promoter species in these catalysts can be seen from the TPR profiles shown in Figs. 8–13. Figure 8 compares the profile for an unpromoted alumina-supported Rh catalyst to that obtained for a catalyst containing 2 wt% Fe. The characteristic profile of the unpromoted system exhibits a broad plateau signifying hydrogen uptake between 100 and 570°C. This feature has been claimed by Yao and co-workers (53) to be due to the migration of the active phase oxide into the subsurface region and the bulk of the support during the calcination step. Recent work carried out in this laboratory (60) suggests that calcination of Al_2O_3-supported Rh at elevated temperatures causes a strong interaction between rhodium and the support. EXAFS data show that the rhodium is present as isolated ions with high coordination to both oxygen and aluminium. In addition to the observed catalytic activities for such reactions as CH_4, CO, and C_3H_6 oxidation and NO reduction by C_3H_6 in the presence of excess oxygen, this is taken as evidence that the noble metal is still exposed at the support surface but present in defect sites in the alumina surface layer. The rhodium is therefore strongly bound and so is difficult to reduce (60).

One might intuitively expect this phenomenon to affect the chemisorption properties of the unpromoted catalyst. However, it can be seen clearly from Fig. 5 that chemisorption of CO and H_2 onto unpromoted alumina-supported Rh appears to be undiminished. This observation also agrees with the findings of Yao *et al.* (53) who have found that the migration of rhodium oxide into the subsurface of the support may be reversed by a subsequent reduction step. Prior to carrying out a chemisorption measurement all our catalysts were reduced in hydrogen for 2 h at 300°C.

Impregnation of 2 wt% Fe into the alumina support followed by a calcination prior to the introduction of Rh to the system has the effect of preventing the Rh from migrating into the support during the final calcination. The characteristic TPR profile for the 2Rh/2Fe/Al shows a single sharp peak centred at 150°C which has been ascribed by Prins and co-workers (58, 59) to the reduction of surface Rh_2O_3 in unpromoted alumina-supported Rh catalysts which had not been pre-calcined.

Figures 9–11 show that the area of this sharp low-temperature reduction feature increases with increasing Fe promoter loading. This suggests that the Rh moiety is accelerating the reduction of the surface iron oxide species. The belief that some of the area of this sharp low temperature peak must be ascribed to reduction of the promoter oxide is strengthened by the fact that no hydrogen consumption is seen to occur in the higher temperature region even for catalysts which possess an elevated promoter loading. Figure 12 shows that for an alumina-supported iron oxide phase (containing no rhodium) a broad feature centred around 400°C and attributable to iron oxide reduction is observed during TPR.

The ability of a noble metal oxide to accelerate the reduction of a second surface metal oxide species with which it is in intimate contact has been reported previously (14, 15, 19, 34, 76, 77). This effect, which has been observed by Prins and co-workers (19) during TPR of MoO_3-promoted SiO_2-supported Rh catalysts has been rationalised in terms of hydrogen spillover. On reduction of Rh_2O_3 to Rh metal, the dissociative chemisorption of H_2 is facilitated. Hydrogen atoms thus formed can spillover and reduce the promoter oxide, resulting in the observed lower reduction temperature.

Further evidence for intimate contact between active phase and promoter in these systems is shown in Fig. 13. It can be seen that the presence of an elevated promoter loading has the effect of increasing the temperature at which reduction of Rh_2O_3 occurs by up to 50°C. Inhibited reduction of Rh_2O_3 by the presence of a promoter oxide has also been reported elsewhere (19, 35, 36, 77, 78) and has been attributed to coverage of the active phase by a layer of promoter oxide which prevents the reductant molecules from reaching the Rh_2O_3.

It is by now clear that the increase in catalytic activity and oxygenate selectivity with increase in promoter loading must be related to the intimate contact between Rh and Fe which is evident from the characterisation experiments. This is consistent with the idea that the active site for oxygenate synthesis occurs at the interface between Rh and oxophilic promoter. Examination of promoted Rh catalysts which are selective for oxygenate synthesis by *in situ* FTIR spectroscopy has shown the existence of an absorption band in the region 1700–1750 cm^{-1} (13, 19, 22, 45, 78).

This band has been assigned to the symmetric stretch of CO which is carbon-bound to Rh and oxygen-bound to the promoter. This mode of CO bonding is known from organometallic chemistry and a review of reactions which form compounds containing bridging carbonyls has been published by Horwitz and Shriver (79). CO bonded in this way has been shown to be activated towards dissociation or

towards the migration of a surface alkyl species, resulting in the formation of a surface acyl species which is considered to be the reactive intermediate in the production of aldehydes and alcohols from synthesis gas (37–45). The enhanced selectivity of the catalysts towards C_2-oxygenates with increasing promoter loading can most likely be explained in terms of optimisation of the area of the active metal promoter oxide interface which is brought about by the close interaction which is evident from chemisorption and TPR measurements.

The decline in the activity of the catalysts for the methanation reaction can also be explained in terms of the build-up of this interface with increasing promoter loading, as it is thought that a large ensemble of reduced Rh metal is required for methanation to proceed efficiently (41, 80). Any increase in the area of this interface must result in a concomitant decrease in the area of exposed reduced Rh metal, thus explaining the observed suppression of CO and H_2 chemisorption as well as the inverse relationship between selectivity to methane and selectivity to ethanol. Ultimately, however, a limiting value is reached where further increase in promoter loading results in the blocking of sites at the rhodium promoter interface. This causes a decrease in the area of this interface which in turn leads to a decrease in the observed oxygenate selectivity. From Figs. 2 and 3 it can be seen that this is exactly what occurs when the Fe-promoter loading of an Al_2O_3-supported Rh catalyst prepared from $Rh(acac)_3$ in toluene is increased from 10 wt% to 14 wt%. Poisoning of the active site for ethanol production results in a decrease in overall catalytic activity and an increase in observed methane selectivity. Overall yield of methane is not affected, further indicating that methanation does not occur at the Rh promoter interface.

This trend towards diminished oxygenated selectivity as the active site is blocked by excess promoter oxide has also been observed by other workers during the study of oxide-promoted Rh catalysts (12, 19, 22, 24, 36, 78).

In conclusion, results are presented in this paper which show that when dealing with preshaped catalyst supports the method of impregnation, the deposited metal oxide precursor, and the rate of drying all have a pronounced effect on the metal oxide distribution of the final catalyst. Results reported on the preparation of Fe-promoted alumina-supported Rh catalysts from various precursors for the production of ethanol from synthesis gas show that similar activities and selectivities for oxygenate synthesis are obtained for all crushed and sieved samples of a given promoter loading, irrespective of the promoter and active metal precursors. This finding is in agreement with that of Wachs and co-workers (31, 48) who claim that the structure and reactivity of a supported metal oxide for a given reaction is not dependent on either the method of preparation or the metal precursor. It is our view, however, that in the case of catalysts made by impregnation from aqueous solutions it is only valid to make this assertion when the support material has been previously crushed and sieved as this allows for a uniform distribution of the metal ions to be more easily achieved.

It has also been shown here that by systematically increasing the promoter loading on the alumina support, a close interaction can be built up between promoter and active metal, giving rise to an increase in the number of interfacial sites on the catalyst surface. This results in ethanol selectivities approaching 50% which, to the best of our knowledge, have not previously been reported for Al_2O_3-supported Rh catalysts. Further promotion of the catalyst system has been shown to be detrimental to ethanol selectivity as the excess promoter oxide has the effect of passively blocking the interfacial sites necessary for oxygenate synthesis.

ACKNOWLEDGMENT

We are grateful to BP Chemicals for providing financial support for this research.

REFERENCES

1. Bhasin, M. M., and O'Connor, G. L., Belgian Patent 824,822, July 28, 1975.
2. Bhasin, M. M., Belgian Patent 824,823, July 28, 1975.
3. Bhasin, M. M., Bartley, W. J., Ellgen, P. C., and Wilson, T. P., *J. Catal.* **54**, 120 (1978).
4. Ichikawa, M., *Bull. Chem. Soc. Japan* **51**(8), 2268 (1978).
5. Ichikawa, M., *Bull. Chem. Soc. Japan* **51**(8), 2273 (1978).
6. Ichikawa, M., *J. Chem. Soc. Chem. Commun.*, 566 (1978).
7. Underwood, R. P., and Bell, A. T., *Appl. Catal.* **21**, 157 (1986).
8. Ichikawa, M., Sekizawa, K., Shikakura, K., and Kawai, M., *J. Mol. Catal.* **11**, 167 (1981).
9. Katzer, J. R., Sleight, A. W., Gajardo, P., Michel, J. B., Gleason, E. F., and McMillan, S., *Faraday Discuss. Chem. Soc.* **72**, 121 (1981).
10. Van der Lee, G., Schuller, B., Post, H., Favre, T. L. F., and Ponec, V., *J. Catal.* **98**, 522 (1986).
11. Van der Lee, G., Bastein, A. G. T. M., Van den Boogert, J., Schuller, B., Luo, H., and Ponec, V., *Faraday Symp. Chem. Soc.* **21**, paper 12 (1986).
12. Kip, B. J., Smeets, P. A. T., Van Grondelle, J., and Prins, R., *Appl. Catal.* **33**, 181 (1987).
13. Kiennemann, A., Breault, R., Hindermann, J. P., and Laurin, M., *J. Chem. Soc. Faraday Trans. 1* **83**, 2119 (1987).
14. Trevino, H., Lei, G. D., and Sachtler, W. M. H., *J. Catal.* **154**, 245 (1995).
15. Schunemann, V., Trevino, H., Lei, G. D., Tomczak, D. C., Sachtler, W. M. H., Fogash, K., and Dumesic, J. A., *J. Catal.* **153**, 144 (1995).
16. Ellgen, P. C., Bartley, W. J., Bhasin, M. M., and Wilson, T. P., *Adv. in Chem.* **178**, 147 (1979).
17. Wilson, T. P., Kasai, P. H., and Ellgen, P. C., *J. Catal.* **69**, 193 (1981).
18. Van den Berg, F. G. A., Glezer, J. H. E., and Sachtler, W. M. H., *J. Catal.* **93**, 340 (1985).
19. Kip, B. J., Hermans, E. G. F., Van Wolput, J. H. M. C., Hermans, N. M. A., Van Grondelle, J., and Prins, R., *Appl. Catal.* **35**, 109 (1987).
20. Bhore, N. A., Sudhakar, C., Bischoff, K. B., Manogue, W. H., and Mills, G. A., *in* "Proceedings, 9th International Congress on Catalysis, Calgary, 1988" (M. J. Phillips and M. Ternan, Eds.), Vol. 2, p. 594, Chem. Institute of Canada, Ottawa, 1988.
21. Guglielminotti, E., Giamello, E., Pinna, F., Strukul, G., Martinengo, S., and Zanderighi, L., *J. Catal.* **146**, 422 (1994).
22. Underwood, R. P., and Bell, A. T., *J. Catal.* **111**, 325 (1988).

23. Y-Hua, D., D-An, C., and K-Rui, T., *Appl. Catal.* **35**, 77 (1987).
24. Luo, H. Y., Bastein, A. G. T. M., Mulder, A. A. J. P., and Ponec, V., *Appl. Catal.* **38**, 241 (1988).
25. Orita, H., Naito, S., and Tamaru, K., *Chem. Lett.* 1161 (1983).
26. Chuang, S. C., Goodwin, J. G., Jr., and Wender, I., *J. Catal.* **95**, 435 (1985).
27. Burch, R., and Petch, M. I., *Appl. Catal.* **88**, 39 (1992).
28. Yoneda, Y., *in* "Progress in C_1 Chemistry in Japan," Elsevier, Amsterdam, 1989.
29. Matsumoto, T., Kim, W. Y., Kishida, M., Nagata, H., and Wakabayashi, K., *Catal. Lett.* **24**, 391 (1994).
30. Ehwald, H., Ewald, H., Gutschick, D., Hermann, M., Miessner, H., Ohlmann, G., and Schierhorn, E., *Appl. Catal.* **76**, 153 (1991).
31. Wachs, I. E., Deo, G., Kim, D. S., Vuurman, M. A., and Hu, H., *in* "Proceedings 10th International Congress on Catalysis, Budapest, 1992" (L. Guczi, F. Solymosi, and P. Tetenyi, Eds.), Vol. A, p. 543, Elsevier, Amsterdam, 1993.
32. Wachs, I. E., and Hardcastle, F. D., *in* "Proceedings, 9th International Congress on Catalysis, Calgary, 1988" (M. J. Phillips and M. Ternan, Eds.), Vol. 3, p. 1449, Chem. Institute of Canada, Ontario, 1988.
33. Turek, A. M., Wachs, I. E., and de Canio, E., *J. Phys. Chem.* **96**, 5000 (1992).
34. Luo, H., Zhou, H., Lin, L., Liang, D., Li, C., Fu, D., and Xin, Q., *J. Catal.* **145**, 235 (1994).
35. Borer, A. L., and Prins, R., *J. Catal.* **144**, 439 (1993).
36. Borer, A. L., Bronnimann, C., and Prins, R., *J. Catal.* **145**, 516 (1994).
37. Bracey, J. D., and Burch, R., *J. Catal.* **86**, 384 (1984).
38. Anderson, J. B. F., Bracey, J. D., and Burch, R., *in* "Proceedings, 8th International Congress on Catalysis, Berlin, 1984," Vol. 5, p. 251, Verlag Chemie, Weinheim, 1984.
39. Rieck, J. S., and Bell, A. T., *J. Catal.* **96**, 88 (1985).
40. Rieck, J. S., and Bell, A. T., *J. Catal.* **99**, 262 (1986).
41. Sachtler, W. M. H., and Ichikawa, M., *J. Phys. Chem.* **90**, 4752 (1986).
42. Sachtler, W. M. H., *in* "Proceedings, 8th International Congress on Catalysis, Berlin, 1984," Vol. 1, p. 151. Dechema, Frankfurt-am-Main, 1984.
43. Sachtler, W. M. H., Shriver, D. F., Hollenberg, W. B., and Lang, A. F., *J. Catal.* **92**, 429 (1985).
44. Sachtler, W. M. H., Shriver, D. F., and Ichikawa, M., *J. Catal.* **99**, 513 (1986).
45. Alekseev, O. S., Beutel, T., Paukshtis, E. A., Ryndin, Yu. A., Likholobov, V. A., and Knozinger, H., *J. Mol. Catal.* **92**, 217 (1994).
46. Vannice, M. A., *J. Catal.* **37**, 449 (1975).
47. Burch, R., and Petch, M. I., *Appl. Catal.* **88**, 61 (1992).
48. Williams, C. C., Ekerdt, J. G., Jehng, J. M., Hardcastle, F. D., Turek, A. M., and Wachs, I. E., *J. Phys. Chem.* **95**, 8781 (1991).
49. Shyr, Y. S., and Ernst, W. R., *J. Catal.* **63**, 425 (1980).
50. Papageorgiou, P., Price, D. M., Gavriilidis, A., and Varma, A., *J. Catal.* **158**, 439 (1996).
51. Stobbe, D. E., van Buren, F. R., Stobbe-Kreemers, A. W., Schokker, J. J., van Dillen, A. J., and Geus, J. W., *J. Chem. Soc. Faraday Trans.* **87**(10), 1623 (1991).
52. Benson, J. E., and Boudart, M., *J. Catal.* **4**, 704 (1965).
53. Yao, H. C., Japar, S., and Shelef, M., *J. Catal.* **50**, 407 (1977).
54. Wanke, S. A., and Dougharty, N. A., *J. Catal.* **24**, 367 (1972).
55. Yang, A. C., and Garland, C. W., *J. Phys. Chem.* **61**, 1504 (1957).
56. Arai, H., and Tominaga, H., *J. Catal.* **43**, 131 (1976).
57. Bond, G. C., *Chem. Soc. Rev.* **20**(4), 441 (1991).
58. Van't Blik, H. F. J., and Prins, R., *J. Catal.* **97**, 188 (1986).
59. Vis, J. C., van't Blik, H. F. J., Huizinga, T., van Grondelle, J., and Prins, R., *J. Catal.* **95**, 333 (1985).
60. Burch, R., Loader, P. K., and Cruise, N. A., *Appl. Catal.*, accepted.
61. Maatman, R. W., and Prater, C. D., *Ind. Eng. Chem.* **49**, 253 (1957).
62. Maatman, R. W., *Ind. Eng. Chem.* **51**, 913 (1959).
63. Komiyama, M., Merrill, R. P., and Harnsberger, H. F., *J. Catal.* **63**, 35 (1980).
64. Komiyama, M., *Catal. Rev.-Sci. Eng.* **27**(2), 341 (1985).
65. Lee, S. Y., and Aris, R., *Catal. Rev.-Sci. Eng.* **27**(2), 207 (1985).
66. Shen, J. Y., Matsuzaki, T., Hanaoka, T., Takeuchi, K., and Sugi, Y., *Catal. Lett.* **28**, 329 (1994).
67. Bastein, A. G. T. M., van den Boogert, W. J., van der Lee, G., Luo, H. Y., Schuller, B., and Ponec, V., *Appl. Catal.* **29**, 243 (1987).
68. Tauster, S. J., Fung, S. C., and Garten, R. L., *J. Am. Chem. Soc.* **100**, 170 (1978).
69. Bond, G. C., and Burch, R., *Catalysis* **6**, 27 (1983).
70. Haller, G. L., and Resasco, D. E., *Adv. Catal.* **36**, 173 (1989).
71. Resasco, D. E., and Haller, G. L., *J. Catal.* **82**, 279 (1983).
72. Haller, G. L., Henrich, V. E., McMillan, M., Resasco, D. E., Sadeghi, H. R., and Sakellson, S., *in* "Proceedings 8th International Congress on Catalysis, Berlin, 1984," Vol. 5, p. 135, Verlag Chemie, Weinheim, 1984.
73. Anderson, J. B. F., Bracey, J. D., Burch, R., and Flambard, A. R., *in* "Proceedings 8th International Congress on Catalysis, Berlin, 1984," Vol. 5, p. 111, Verlag Chemie, Weinheim, 1984.
74. Morris, S., Moyes, R., and Wells, P. B., *Stud. Surf. Sci. Catal.* **11**, 247 (1982).
75. Anderson, J. B. F., Burch, R., and Cairns, J. A., *Appl. Catal.* **21**, 179 (1986).
76. Burch, R., *J. Catal.* **71**, 348 (1981).
77. Van't Blik, H. F. J., and Niemantsverdriet, J. W., *Appl. Catal.* **10**, 155 (1984).
78. Underwood, R., and Bell, A. T., *J. Catal.* **109**, 61 (1988).
79. Horwitz, C. P., and Shriver, D. F., *Adv. Organomet. Chem.* **23**, 219 (1984).
80. Kawai, M., Uda, M., and Ichikawa, M., *J. Phys. Chem.* **89**(9), 1654 (1985).